Abdominal Imaging

Published online: 8 March 2005

Abdom Imaging (2005) 30:249–258
DOI: 10.1007/s00261-004-0223-2

INVITED UPDATE

Multislice CT virtual angioscopy of the abdomen

P. Carrascosa,[1] C. Capuñay,[1] M. Vembar,[2] L. Ciancibello,[2] J. Carrascosa[1]

[1]Diagnóstico Maipú, Alsina 30, San Isidro, 1642 Buenos Aires, Argentina
[2]Philips Medical Systems, 595 Miner Road, Highland Heights, Cleveland, OH 44143, USA

Abstract

Background: Computed tomographic (CT) angiography represents an important clinical tool in the evaluation of vascular disorders. Virtual angioscopy can be reconstructed with volumetric CT data sets. We evaluated the feasibility and clinical value of this application in the assessment of abdominal vessels.
Methods: Data sets of CT angiographic studies obtained with helical (n = 120) and multislice (n = 180) CT scanners were analyzed on a workstation for postprocessing. Vascular evaluation was done on conventional enhanced axial images, three-dimensional reconstructions, and virtual angioscopic images.
Results: We made 123 studies in patients without aortic disease. Of the patients evaluated for stent-graft treatment, 63 showed normal patency, seven had partial thrombosis of the stent-graft, five showed total occlusion of the stent-graft, and 10 had leaks. From the 92 remaining CT studies, 63 vascular aneurysms and nine dissections were diagnosed.
Conclusion: The current technology produces high-quality virtual angioscopic images. Although axial and multiplanar views are usually adequate for detecting a vascular disorder, virtual angioscopic views better define anatomic details.

Key words: Multislice computed tomography—Computed tomographic angiography—Virtual angioscopy—Abdominal vessels—Abdominal aorta—Computer-assisted diagnosis

Computed tomographic angiography (CTA) is an important clinical diagnostic tool for the evaluation of vascular disorders and a well-known, accurate, noninvasive technique for the diagnosis of abdominal artery disorders [1]. Virtual angioscopy (VA) is a computer-generated simulation of endoscopic images derived from three-dimensional (3D) CT data sets [2, 3]. This technique allows exploration of the inner surfaces of the aorta and its branches. This information can be helpful in the evaluation of different pathologic entities and in some cases can add important useful details for the final diagnosis.

We evaluated the feasibility and clinical value of this application in the assessment of the abdominal vessels.

Material and methods

We retrospectively reviewed CTA data sets from 300 patients (235 male, 65 female; age range 21–84 years) imaged for the study of the aorta or its branches.

One hundred twenty studies were performed on a helical CT scanner (PQ 5000, Picker International, Inc., Cleveland, OH, USA) using the following parameters: 4-mm slice thickness, 2-mm reconstruction interval, pitch of 2, 170 mAs/slice, 120 kV, and 512 × 512 matrix. The remaining studies were performed on a four-row CT scanner (Mx 8000, Philips Medical Systems, Cleveland, OH, USA) using 3.2-mm slice thickness, 1.6-mm reconstruction interval, pitch of 1.25, 180 mAs/slice, 120 kV, 0.75-s rotation time, and 512 × 512 matrix.

The patient was instructed in a breath-hold technique. The helical CT scanner required a 30- to 40-s breath-hold. Newer multislice CT scanners are faster, and a breath hold of only 20 s was needed.

A 20-gauge intravenous catheter was placed into an antecubital vein. A 120-mL bolus of iodinated contrast medium was injected with an automatic power injector at rate of 4 mL/s. CT acquisition of image data was initiated after a preset empirical delay of 20 to 25 s after the start of the contrast material injection.

All data sets were reprocessed on a CT workstation (MxView, Philips Medical Systems). 3D postprocessing techniques were used to produce images that simulate conventional angiograms. These techniques include maximum intensity projection, volume rendering, and multiplanar reconstruction (MPR). These CT data sets were also used to create intraluminal images, therby generating virtual vascular endoscopic studies.

Correspondence to: P. Carrascosa; *email:* investigacion@diagnosticomaipu.com.ar

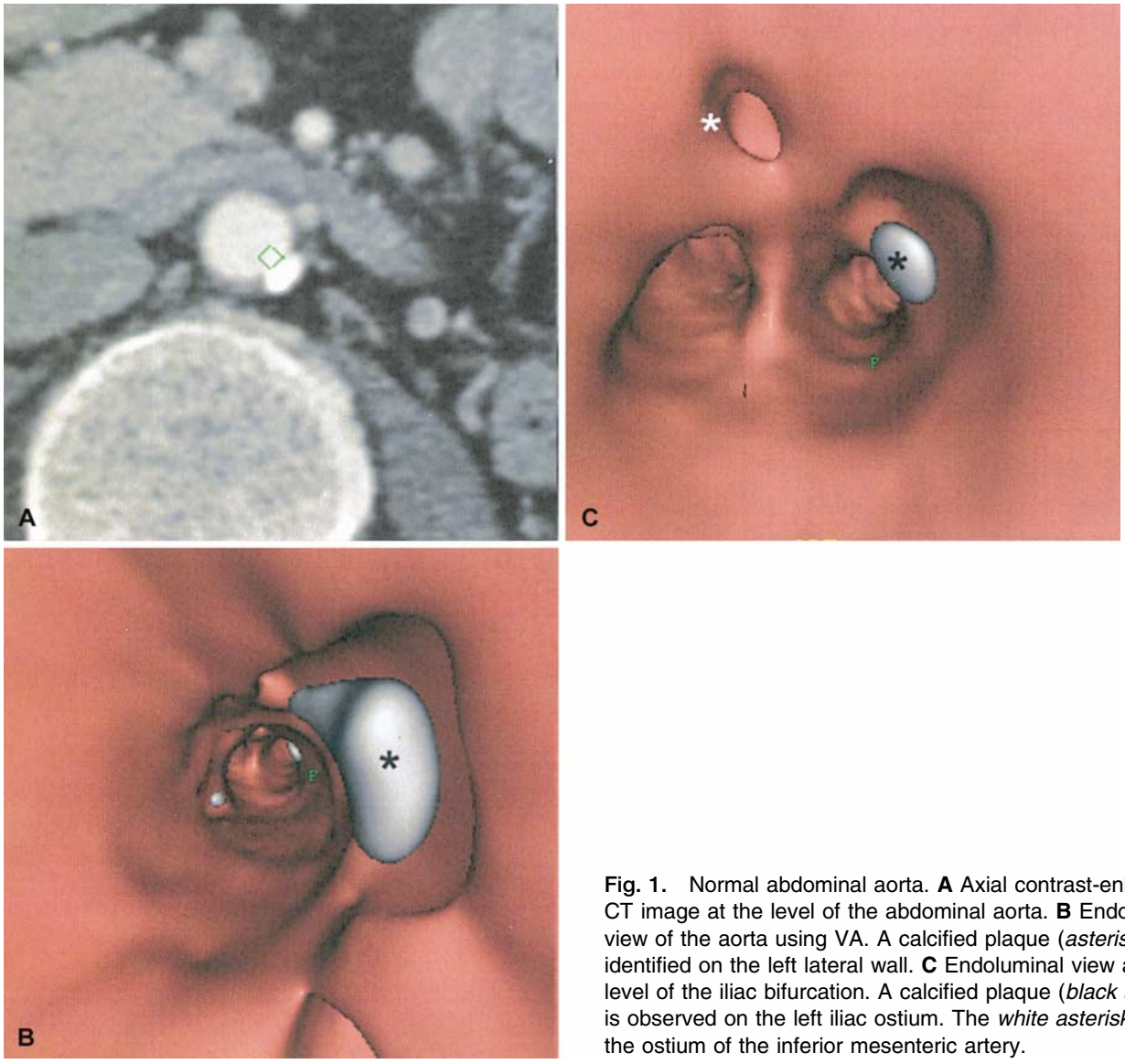

Fig. 1. Normal abdominal aorta. **A** Axial contrast-enhanced CT image at the level of the abdominal aorta. **B** Endoluminal view of the aorta using VA. A calcified plaque (*asterisk*) is identified on the left lateral wall. **C** Endoluminal view at the level of the iliac bifurcation. A calcified plaque (*black asterisk*) is observed on the left iliac ostium. The *white asterisk* marks the ostium of the inferior mesenteric artery.

Results

Of 300 studies, 123 (41%) showed an aorta without evidence of severe atherosclerotic disease, aortic aneurysm or dissection (Fig. 1), or any vascular disorder in other abdominal vessels.

In 83 patients, CTA diagnosed the presence of a vascular aneurysm (45 aortic aneurysms, 24 aortoiliac aneurysms, eight iliac arteries, four renal arteries, one celiac trunk, and one splenic artery).

The diagnosis of aortic dissection was made in nine cases.

Eighty-five patients underwent CTA after treatment of aortic or aortoiliac aneurysms with endoluminal stent-grafts.

Any occlusion of a major aortic branch was diagnosed in our study population.

Graft thrombosis is an infrequently reported condition. Seven partial thromboses of the stent-graft and five total thromboses of one graft limb were diagnosed.

Perigraft leakage has been defined as the persistence of blood flow outside the lumen of the endoluminal graft but within the aneurysm sac [1]. A non–graft-related leakage caused by persistent blood flow into the aneurysm sac was seen in seven patients. The leak was caused by flow from a patent inferior mesenteric artery in five patients and by flow from patent lumbar arteries in two. Three leaks related to the stent-graft also were diagnosed.

Discussion

CTA is a noninvasive, accurate diagnostic technique for evaluation of abdominal arteries. The volumetric data allow clear delineation of the aorta and branch vessels.

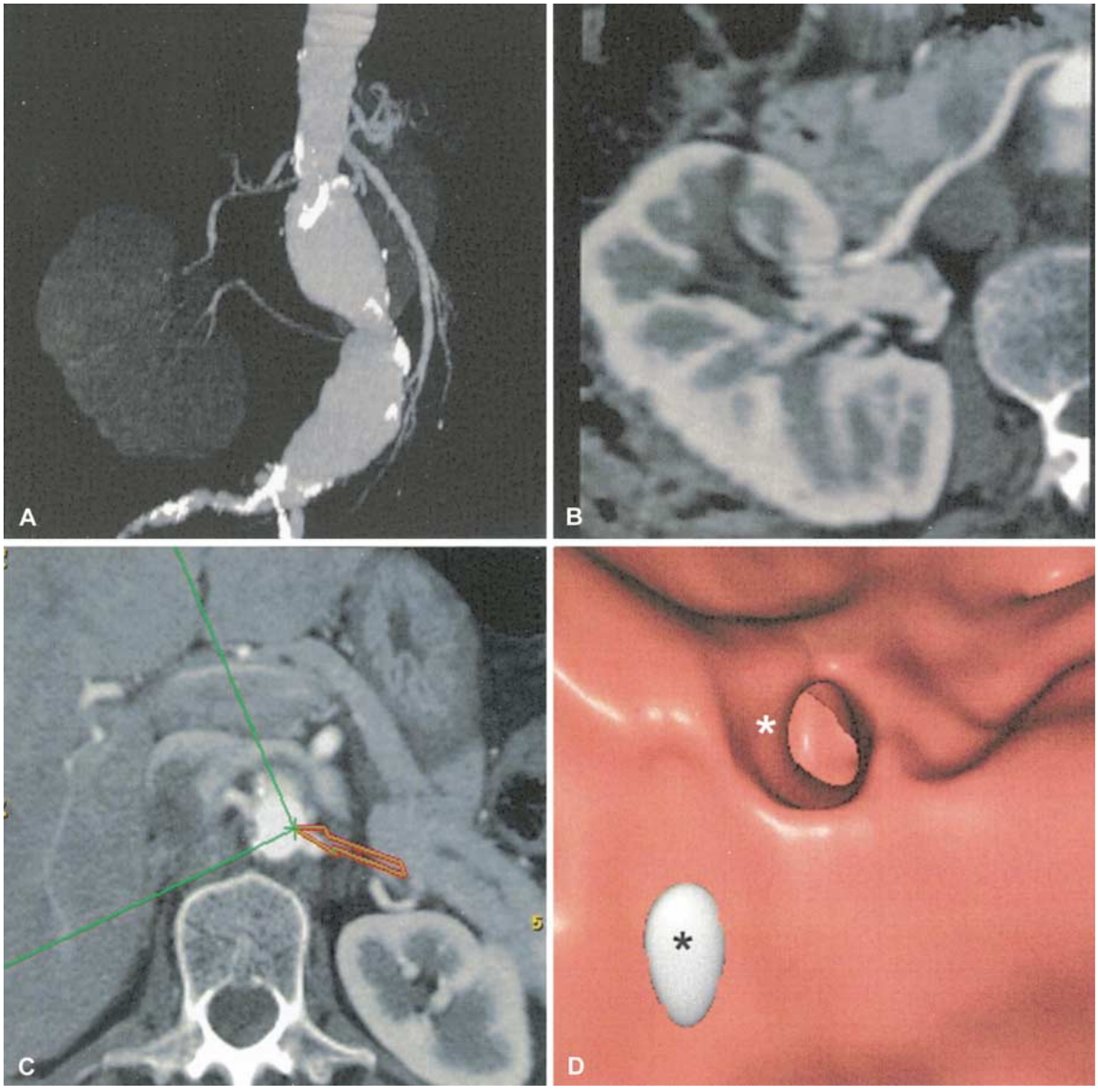

Fig. 2. CTA of the right renal artery. **A** Maximum intensity projection coronal image of the abdominal aorta. **B** Curved MPR image of the right renal artery. **C** Axial image at the level of the right renal ostium. **D** VA view of the ostium of the right renal artery (*white asterisk*) and calcified plaque (*black asterisk*).

VA has been recently introduced into clinical medicine. With this technique, it is possible to create endoluminal views and ''fly through'' a vessel by using the data sets obtained by CT scans. It provides a comprehensive delineation of the lumen and allows understanding the effects of disease on it. For this modality of postprocessing, special software is required to create the inner surface of the vessel that simulates the endoscopic view.

Normal aorta

The main application in this group of patients is the assessment of the ostia of the aortic branches (Fig. 2). It is helpful for the identification of accessory renal arteries and detection of anatomic variations [4, 5] (Fig. 3).

Aortic dissection

In these patients, the false and true lumens were visualized. VA clearly demonstrated the relation between the true and false luminal flow channels and the aortic branches and enabled correct visualization of the intimal flap and, in some cases, of its origin [6]. A correlation with MPR images allowed better interpretation of the VA views (Fig. 4).

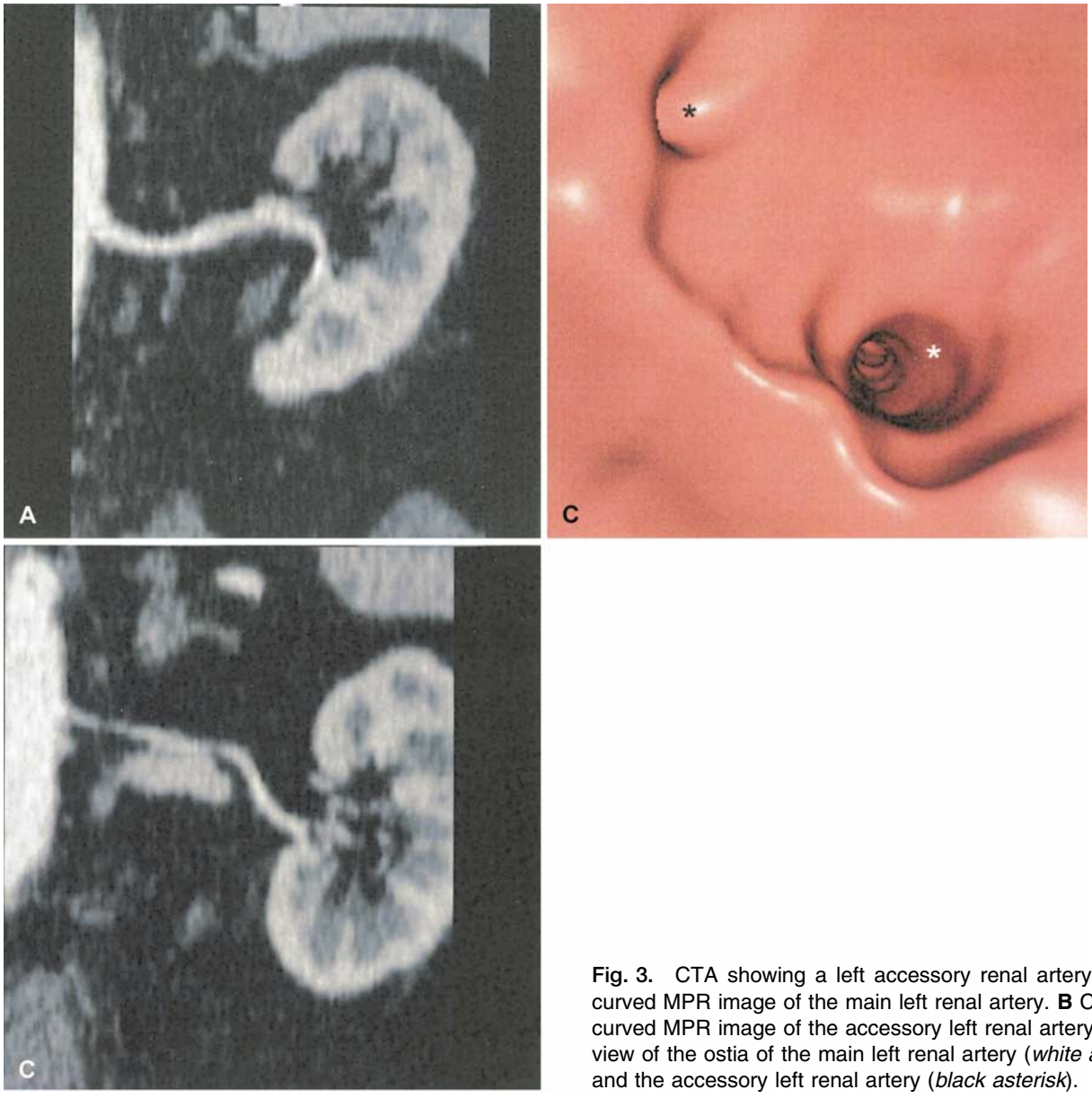

Fig. 3. CTA showing a left accessory renal artery. **A** Coronal curved MPR image of the main left renal artery. **B** Coronal curved MPR image of the accessory left renal artery. **C** VA view of the ostia of the main left renal artery (*white asterisk*) and the accessory left renal artery (*black asterisk*).

Stent-graft therapy

Stent-graft therapy is a safe, effective procedure for the treatment of abdominal aortic aneurysms [1, 7] as an alternative for open surgical repair.

CTA is the current diagnostic modality of choice for posttreatment evaluation [8]. MPR images and maximum intensity projections are the two most useful postprocessing techniques. VA views clearly depict the proximal and distal segments of the endovascular graft and its relation to the ostia of the renal arteries (Fig. 5), the exact location of an endovascular leakage, and the integrity of the graft and its patency (Fig. 6). VA also can be used to evaluate the artery wall by demonstrating irregularities of the luminal surface.

Aneurysm

CTA is the diagnostic modality of choice for the pretreatment evaluation of abdominal aortic aneurysms. This procedure allows a complete description of the aneurysm, its length, its diameters, and the characteristics of its walls. In this regard, VA images play a complementary role. It easily delimits the relations between the proximal aneurysmal neck and the origin of the renal arteries, compromise of the iliac branches, and distribution of atherosclerotic plaques on the wall.

VA was accurate in detecting complex lesions with irregular surfaces and calcification. In contrast, noncalcified plaques with a density close to the vessel wall were poorly visualized. They were identified because they

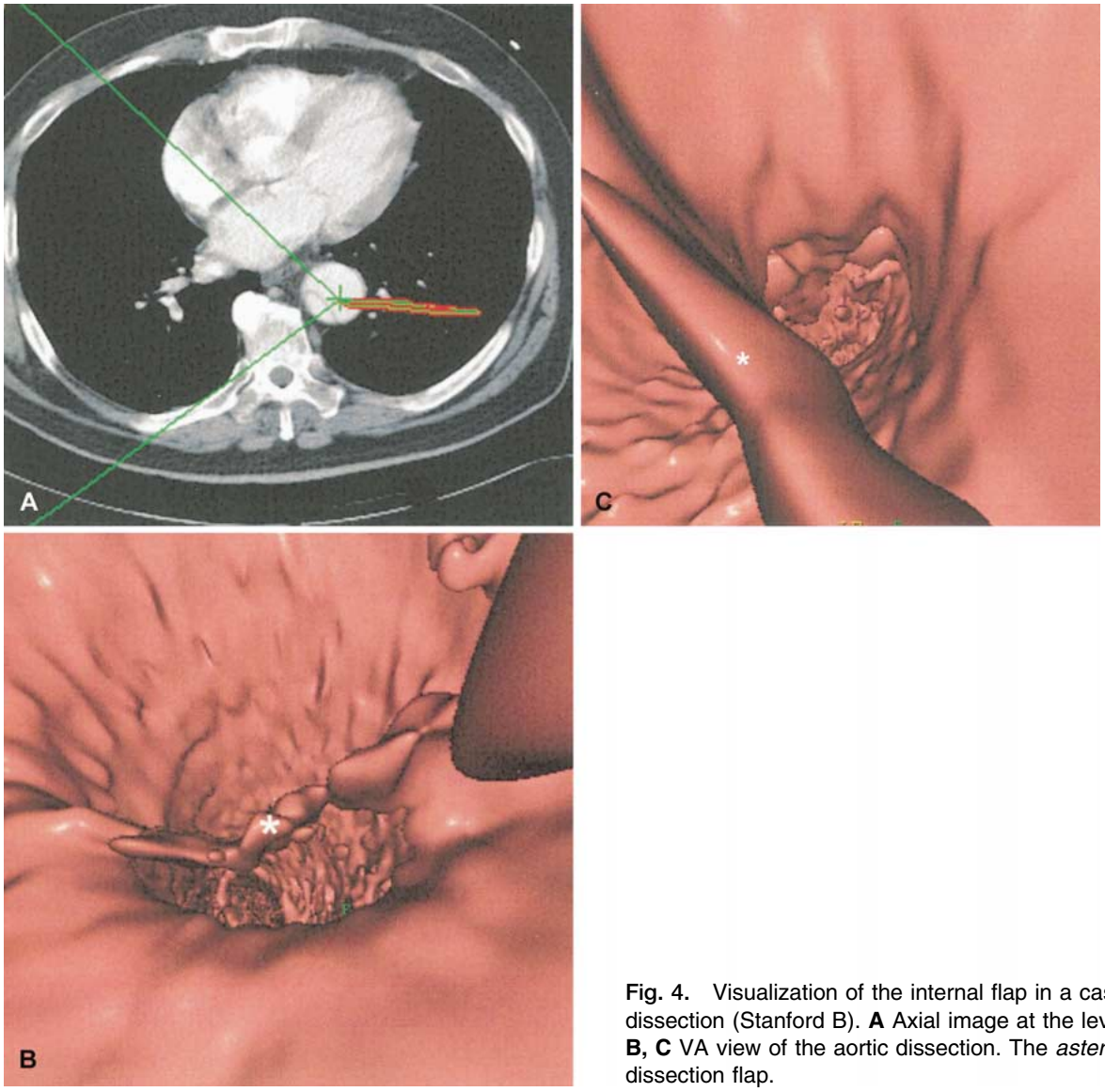

Fig. 4. Visualization of the internal flap in a case of aortic dissection (Stanford B). **A** Axial image at the level of the flap. **B, C** VA view of the aortic dissection. The *asterisk* marks the dissection flap.

caused significant luminal narrowing (Fig. 7). Further, conventional contrast-enhanced axial images and MPR reformats were superior to VA for noncalcified lesion detection.

Evaluation of other artery aneurysms, such as of the celiac trunk or splenic artery, also can be performed with VA (Figs. 8, 9).

Conclusion

CTA is a safe, fast, noninvasive imaging technique for the evaluation of abdominal vessels. The use of a maximum intensity projection technique often clarifies the anatomy of the aorta and branch vessels. Current 3D postprocessing software for CTA data sets allows reconstruction of VA images with good image quality. With a larger anatomic view of the artery lumen, this technique clearly shows the relations of the stent-graft and the branch vessels and visualizes intimal flap in a vascular dissection and characteristics of the inner surface of the vascular wall in atherosclerotic disease. VA was accurate in detecting complex lesions because of the high density of calcium deposits. Further technical innovations and improved postprocessing software are necessary to allow a more precise angioscopic view of the vascular wall.

Acknowledgements. P. Carrascosa, M. Vembar, and L. Ciancibello received financial support from Philips Medical Systems, Cleveland, Ohio, USA.

References

1. Tillich M, Hausegger KA, Tiesenhausen K, et al. (1999) Helical CT angiography of stent-grafts in abdominal aortic aneurysms: morphologic changes and complications. Radiographics 19:1573–1583

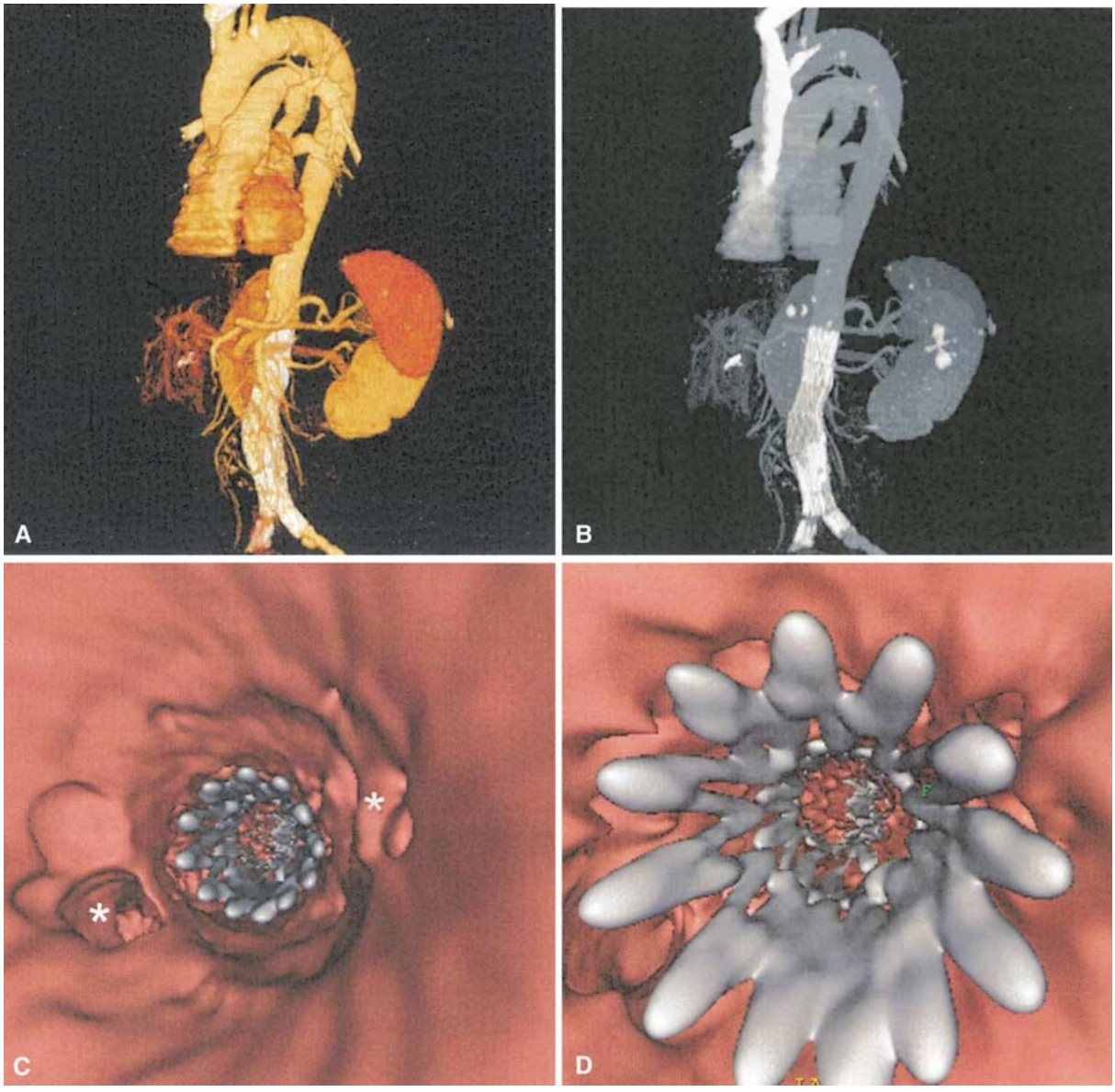

Fig. 5. Aortoiliac stent-graft follow-up by CTA. **A** 3D volume-rendered reconstruction of the aorta. **B** Maximum intensity projection image of the aorta. **C** VA view of the abdominal aorta. *Asterisks* mark ostia of the renal arteries. **D** VA view at the level of the stent-graft.

2. Schroeder S, Cop AF, Ohnesorge B, et al. (2002) Virtual coronary angioscopy using multislice computed tomography. Heart 87:205–209
3. Neri E, Bonanomi G, Vignali C, et al. (2000) Spiral CT virtual endoscopy of abdominal arteries: clinical applications. Abdom Imaging 25:59–61
4. Neri E, Caramella D, Bisogni C, et al. (1998) Detection of accessory renal arteries with virtual vascular endoscopy of the aorta. Cardiovasc Intervent Radiol 22:1–6
5. Urban BA, Ratner LE, Fishman EK (2001) Three-dimensional volume-rendered CT angiography of the renal arteries and veins: normal anatomy, variants, and clinical applications. Radiographics 21:373–386
6. Sbragia P, Neri E, Panconi M, et al. (2001) CT virtual angioscopy in the study of thoracic aortic dissection. Radiol Med 102:245–249
7. Blum U, Langer M, Spillner G, et al. (1996) Abdominal aortic aneurysms: preliminary technical and clinical results with transfemoral placement of endovascular self-expanding stent-grafts. Radiology 198:25–31
8. Armerding MD, Rubin GD, Beaulieu CF, et al. (2000) Aortic aneurysmal disease: assessment of stent-graft treatment—CT versus conventional angiography. Radiology 215:138–146

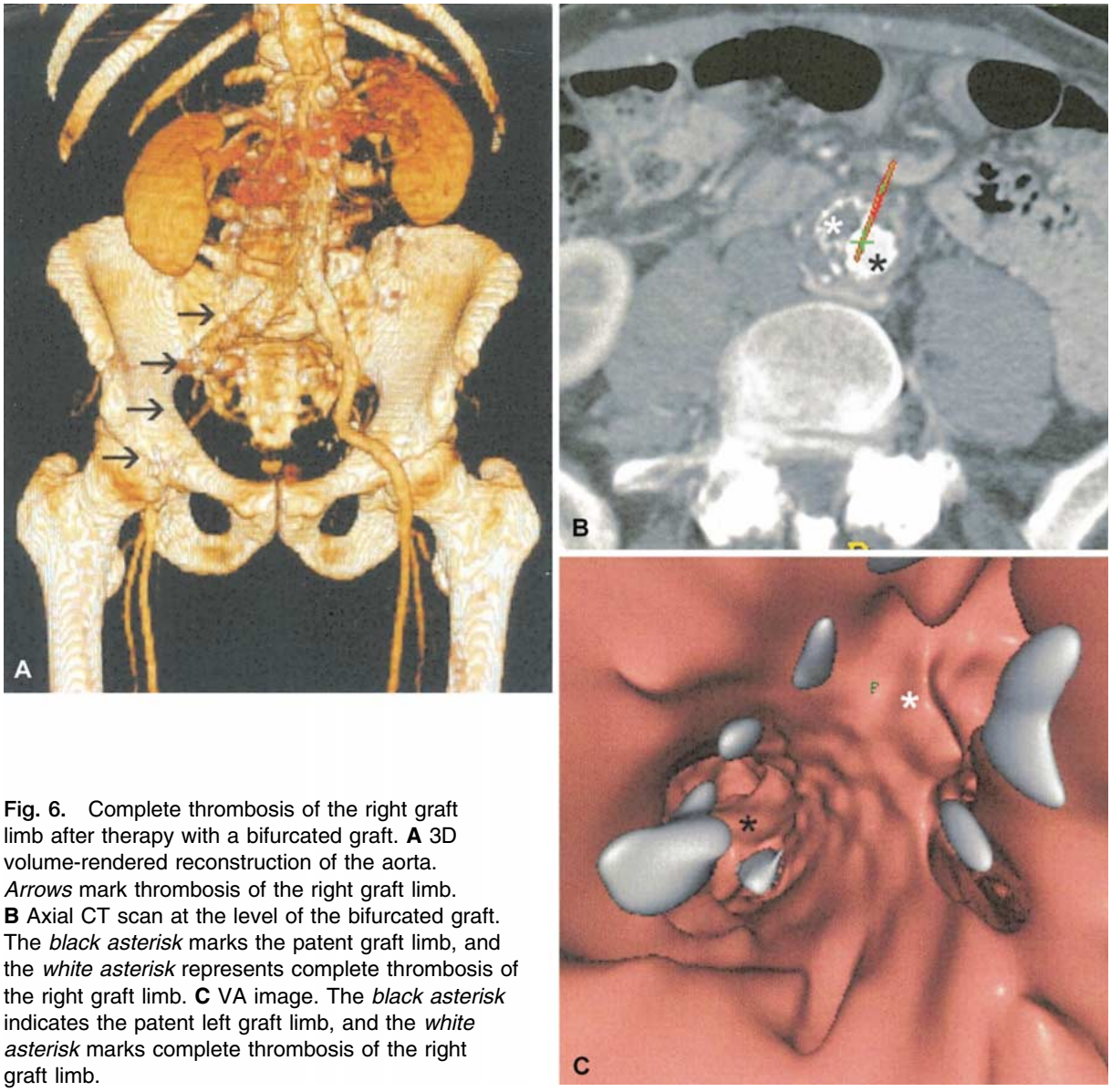

Fig. 6. Complete thrombosis of the right graft limb after therapy with a bifurcated graft. **A** 3D volume-rendered reconstruction of the aorta. *Arrows* mark thrombosis of the right graft limb. **B** Axial CT scan at the level of the bifurcated graft. The *black asterisk* marks the patent graft limb, and the *white asterisk* represents complete thrombosis of the right graft limb. **C** VA image. The *black asterisk* indicates the patent left graft limb, and the *white asterisk* marks complete thrombosis of the right graft limb.

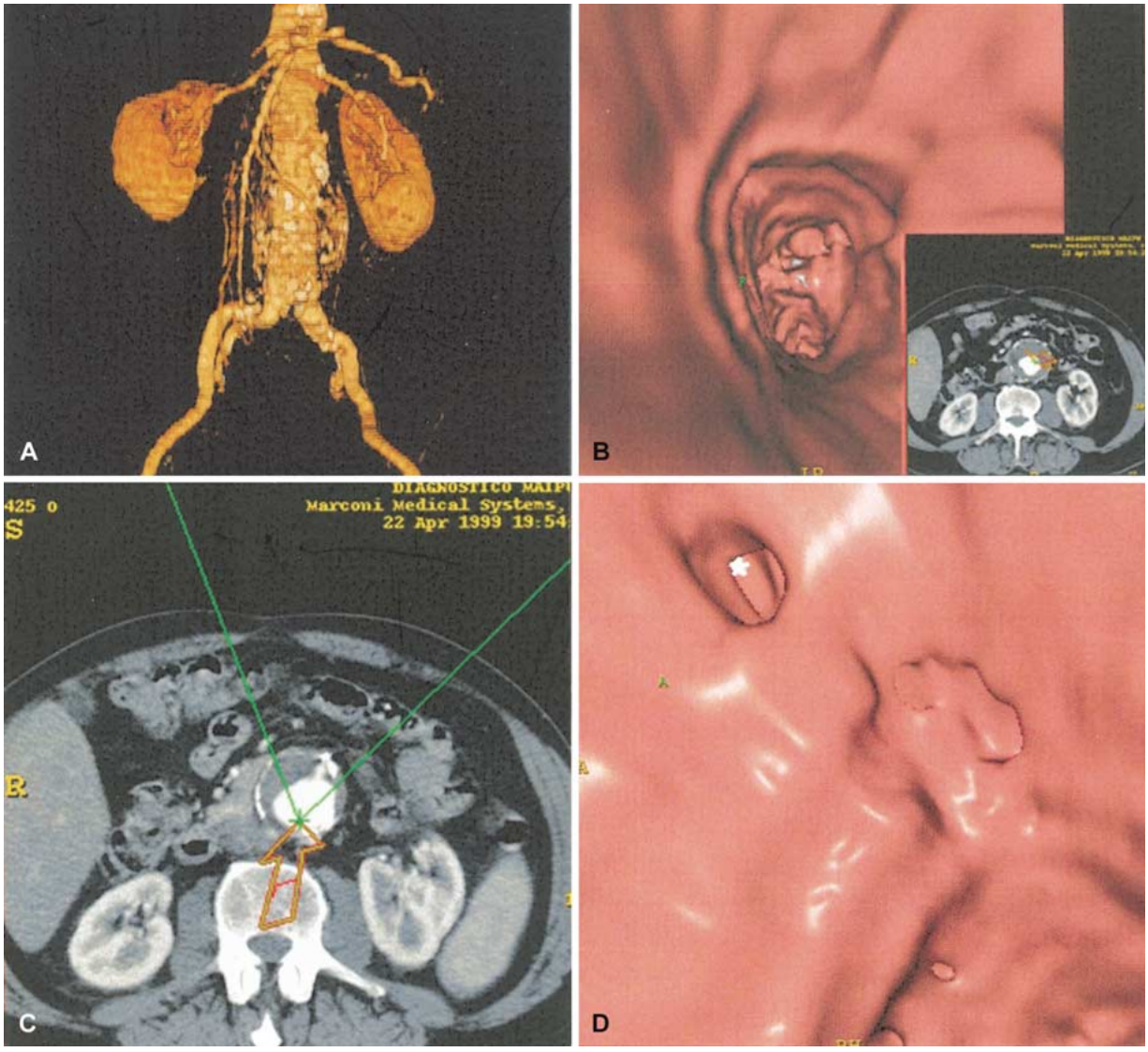

Fig. 7. CTA demonstrating an aortic aneurysm that is partly thrombosed. **A** 3D volume-rendered reconstruction of the aorta. **B** VA shows significant luminal narrowing due to a parietal thrombosis. **C** Axial CT image at the level of the origin of the inferior mesenteric artery. **D** VA image at the level of the origin of the inferior mesenteric artery (*asterisk*).

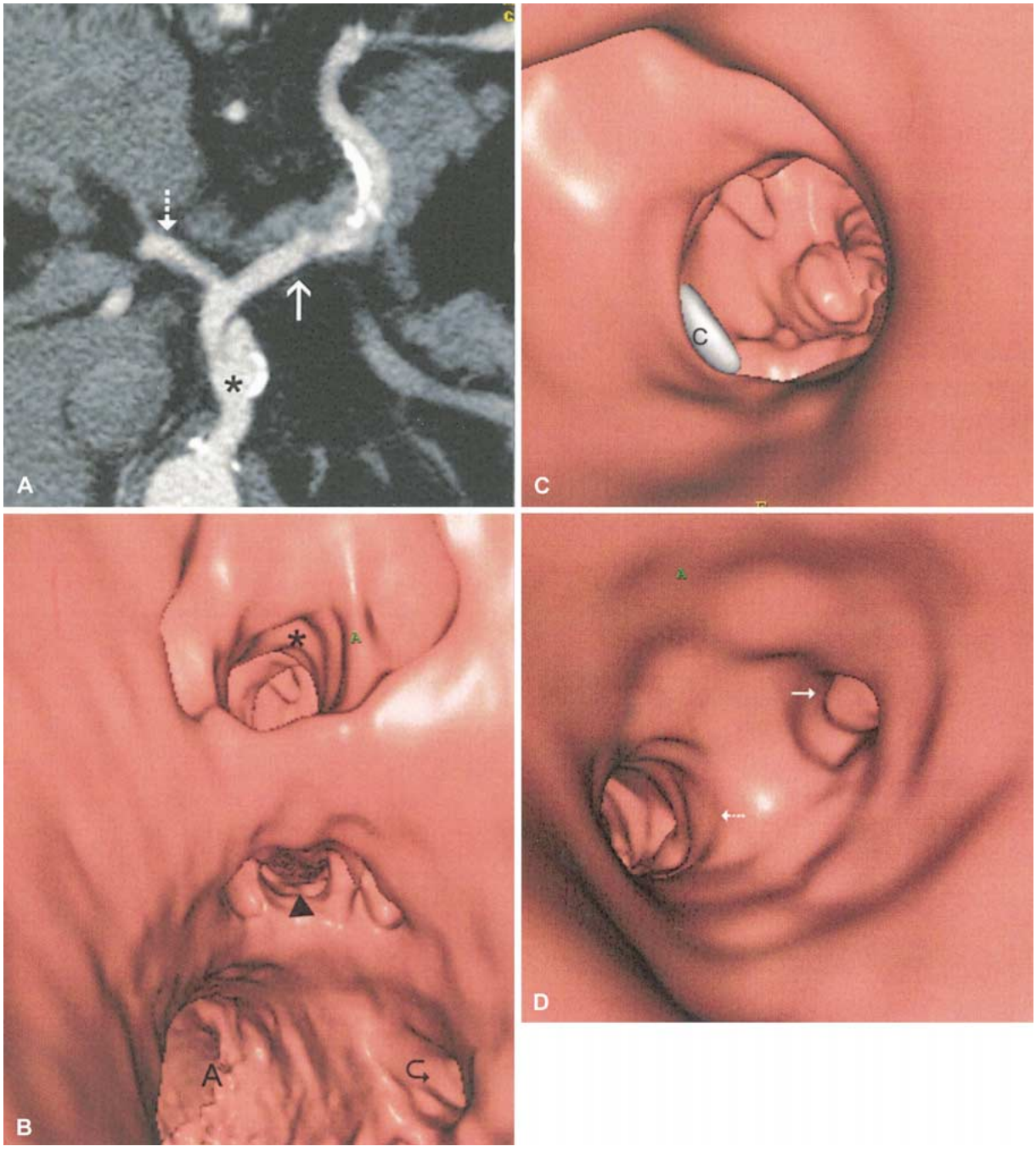

Fig. 8. CTA depicting a celiac trunk aneurysm. **A** Curved MPR image of the celiac trunk. **B** VA image at the level of the origin of the celiac trunk and superior mesenteric artery. **C** VA image at the level of the celiac trunk aneurysm. **D** VA image at the level of the celiac trunk bifurcation. *Asterisk* celiac trunk, *solid arrow* splenic artery, *dashed arrow* hepatic artery, *arrowhead* superior mesenteric artery ostium, *curved arrow* left renal artery ostium, *A* aortic lumen, *C* calcified plaque.

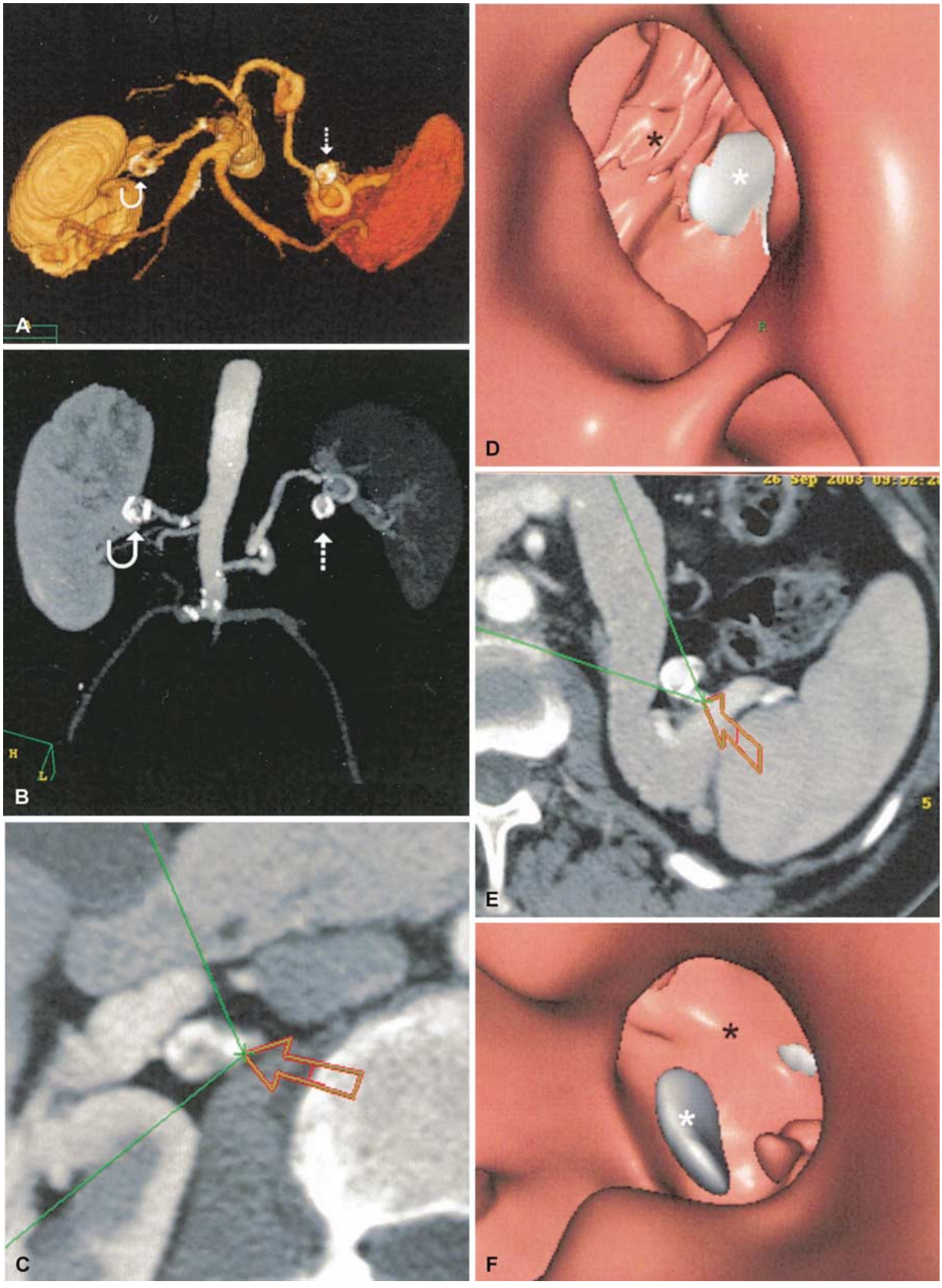

Fig. 9. Aneurysmatic dilatation of the middle segment of the right renal artery (*curved arrow*) and splenic artery (*dashed arrow*). **A** Axial volume-rendered reconstruction image. **B** Coronal maximum intensity projection reconstruction image. **C** Axial contrast-enhanced CT image at the level of the right renal artery aneurysm. **D** VA view. **E** Axial contrast-enhanced CT image at the level of the splenic artery aneurysm. **F** VA view. *Black asterisk* vascular lumen, *white asterisk* calcified plaque.